Available online at www.sciencedirect.com
ScienceDirect
Journal of Power Sources 170 (2007) 441–449
JOURNAL OF POWER SOURCES
www.elsevier.com/locate/jpowsour

New composite electrodes made of polypyrrole and graphite: Construction, optimization and characterization

G. Dione [a,b], M.M. Dieng [a], J.J. Aaron [b,*], H. Cachet [c], C. Cachet [c]

[a] *Département de Chimie, Faculté des Sciences et Techniques, Université Cheikh Anta Diop, Dakar-Fann, Senegal*
[b] *Interfaces Traitement Organisation et Dynamique des Systèmes (ITODYS), de l'Université Paris 7-Denis Diderot, Associé au CNRS UMR 7086, 1, rue Guy de la Brosse, 75005 Paris, France*
[c] *Laboratoire des Interfaces et Systèmes Electrochimiques, UPR 15 CNRS, Associé à l'Université Paris 6, 4, Place Jussieu, 75252 Paris, France*

Received 5 January 2006; received in revised form 31 October 2006; accepted 7 February 2007
Available online 5 May 2007

Abstract

In this work, new composite electrodes were developed, optimized and characterized for possible, future use in batteries and/or super-capacitors. These composite electrodes were prepared from chemically synthesized polypyrrole (Ppy), graphite carbon and Teflon and their physico-chemical performances were tested using different techniques. Their conductivity and porosity were investigated under various conditions. Their macroporous structure was also studied by the BET method. Two distinct electrochemical reactions were found to take place at these electrodes, including a redox reaction with insertion and expulsion of anions, and a capacitive reaction at the electrode/electrolyte interface. The specific capacity, experimentally obtained with an electrode containing 40 wt% of Ppy (99.6 mAh g^{-1}), was larger than the theoretical one, due to double-layer effects at the Ppy/electrolyte interface. The double-layer capacitance at the electrode/electrolyte interface of the composite electrodes, investigated by electrochemical impedance spectroscopy, was found to represent at most 0.1% of the total electrode capacitance.

Keywords: Composite electrodes; Polypyrrole; Graphite; Cyclic voltammetry; Electrochemical impedance spectroscopy

1. Introduction

As a consequence of numerous, potential applications, the research efforts on conductive polymers have considerably increased in recent years. For instance, polypyrrole (Ppy) is currently considered as one of the most promising materials for the development of advanced batteries, due to its good conductivity and stability. One of the most interesting characteristics of these conductive polymers is their capacity to store electrical charge, which can be recovered upon demand. This makes them good candidates as components of advanced rechargeable batteries or super-capacitors [1–4]. These batteries can operate when the ions interchange easily between the electrolytic solution and the electrodes [5]. In fact, the ions direction depends on both the electrode nature (anode or cathode) and the electrochemical reaction (charge or discharge) [6].

Different materials have been proposed to build these electrodes. Generally, in order to increase the charge, to lower the electrode weight and to make easier the anions interchange, these materials have to be conductive and porous. The use of carbon paste electrodes in electrochemical studies has already been described in other studies [7–9]. The combination of carbon (graphite) and a conductive polymer such as Ppy also should be an effective way to obtain a good composite electrode, fulfilling the above-requested conditions. The fabrication of a Ppy/graphite composite electrode, with interesting capacitance and conductivity properties, has been reported by electrochemical polymerization of pyrrole (py) on the surface of graphite fiber [10,11]. In order to increase the active surface of the electrode substrate, some authors have simultaneously electrodeposited Ppy and carbon nanotubes [12,13]. However, electropolymerization seems to be less efficient than chemical polymerization for the production of important masses of composite electrodes and for the preparation of relatively thick polymer films. Recently, Park et al. [14] have built Ppy/graphite electrodes with a rather high specific capacitance by chemical polymerization of py on

* Corresponding author. Tel.: +33 1 44 27 69 62; fax: +33 1 44 27 68 14.
E-mail address: aaron@paris7.jussieu.fr (J.J. Aaron).

0378-7753/$ – see front matter © 2007 Elsevier B.V. All rights reserved.
doi:10.1016/j.jpowsour.2007.02.092

the surface of a porous graphite fiber matrix, using an elegant, sequential dipping method.

In the present work, we have developed a new type of large surface composite electrodes, made of graphite carbon and chemically synthesized Ppy in percentages up to 70 wt%. Since these composite electrodes can be used as an active matter in batteries or super-capacitors, we have decided to precisely evaluate their relevant physico-chemical and electrochemical properties by means of cyclic voltammetry (CV), chronopotentiometry, electrochemical impedance spectroscopy (EIS) and other techniques.

2. Experimental

Ppy was synthesized by oxidizing pyrrole in water with ferric perchlorate $Fe(ClO_4)_3$, according to the procedure of Mermilliod et al. [15]. An amount of pyrrole corresponding to a 0.3 M concentration was mixed with distilled water. The resulting emulsion was cooled down at 0 °C. A 0.7 M $Fe(ClO_4)_3{\cdot}9H_2O$ (Aldrich) aqueous solution was also prepared, degassed and cooled. When the latter solution and the pyrrole emulsion were admitted to contact, a black precipitate of Ppy immediately appeared. The mixture was kept at 0 °C and continuously stirred for about 1 h, then rinsed with water and thoroughly spun-dry. Afterwards, it was washed with dry acetonitrile and dried in a glove box.

For the preparation of composite electrodes, the Ppy powder was mixed with graphite carbon and a small quantity of Teflon as binder, and the obtained Ppy/graphite composite material was homogenized and then pressed to obtain pellets. These pellets were prepared by pressing the composite material (100 or 200 mg) under pressures going from 0.5 to 2.0 tonnes cm^{-2}, using a KBr tablet mould in a Carver Laboratory press model S/N 3392-69. The prepared pellets which had a 1 cm^2 area and about 1 mm thickness were inserted into a working electrode, with an inox collector, as described in Fig. 1.

All electrochemical measurements were carried out in a 0.3 M $NaClO_4$ aqueous solution, using a standard three-electrode cell, controlled by an EG&G potentiostat 362. The electrochemical cell was constituted of a platinum grid as counter-electrode, a saturated calomel electrode as reference electrode, and a composite electrode as working electrode (Fig. 2).

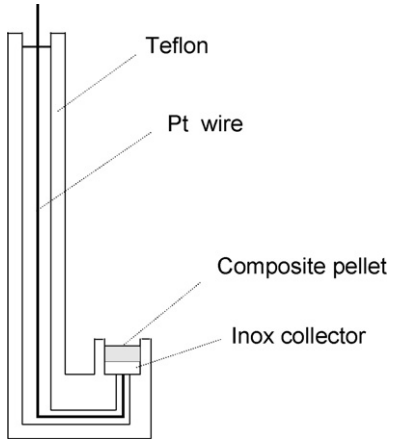

Fig. 1. Schematic view of the composite electrode.

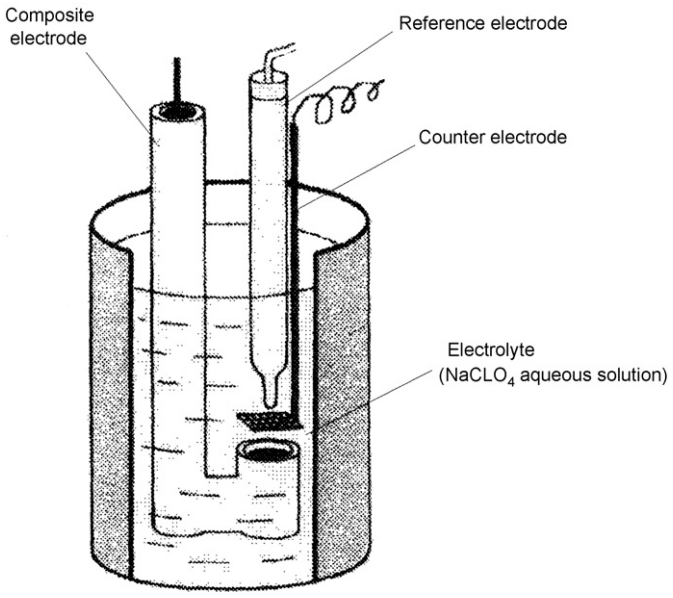

Fig. 2. The electrochemical cell.

The electrical conductivity of the Ppy/graphite composite material was determined at room temperature (298 K) by a four-probe method, with a constant courant value of 1 μA, and the porosity was evaluated after immersion of the material during 48 h into a 0.3 M $NaClO_4$ aqueous solution.

For the BET measurements, the N_2 adsorption–desorption isotherms were collected on a Micromeritics ASAP 2010 analyzer. Prior BET analysis, the samples were degassed (pressure < 1 Pa) at 423 K during 12 h. The surface areas, pore volume and size were evaluated by means of the BET method.

The scanning electron microscopy (SEM) photos of the surface of composite material pellets were made on a S 440 model Leica instrument equipped with a tungsten filament, using a four-sector detector for secondary and retro-diffused electrons.

Electrochemical impedance spectroscopy (EIS) measurements were performed using a frequency response analyzer (Solartron 1250) and a potentiostat (Solartron 1286), controlled by the FRA™ software. The applied ac signal was 10 mV. Quasi steady-state polarization curves were obtained under potentiostatic control. Starting from +600 mV/SCE, the potential was decreased by step of 50 mV down to −800 mV/SCE. At every step, after waiting for 10 mn, the current was determined before and after the electrode impedance to be measured between 62 kHz and 4 mHz.

3. Results and discussion

3.1. Effect of the pressure on the conductivity of Ppy/graphite pellets

The pressure dependence of the conductivity of Ppy/graphite pellets was examined in the range of 0.5–2 tonnes cm^{-2} for

composite electrodes containing 10 wt% of Ppy. We found that the conductivity strongly increased with pressure from about 0.70 to 1.45 S cm^{-1}, until a pressure value of approximately 1.7 tonnes cm^{-2}, and then reached a plateau region, remaining constant between 1.7 and 2.0 tonnes cm^{-2}. For this reason, a value of 2.0 tonnes cm^{-2} was retained for pressing the pellets throughout this work.

3.2. Effect of Ppy concentration on the electrical conductivity

The effect of varying the Ppy concentration in the composite electrode on the electrical conductivity was investigated. We observed that the surface conductivity rapidly diminished from about 1.5 to 0.7 S cm^{-1}, when the Ppy weight fraction increased from 10 to 50 wt%. This significant decrease of the composite electrode conductivity, occurring at the higher Ppy percentages, can be explained by the conductivity of Ppy pellets (0.028 S cm^{-1}) much smaller than that of graphite (2.10 S cm^{-1}) [16].

3.3. Porosity of Ppy/graphite composite electrodes

Porosity was defined as the amount of electrolyte retained in the composite electrode after a 48 h immersion time in a 0.3 M $NaClO_4$ aqueous solution. The amount of electrolyte (μ), expressed in mg g^{-1}, was evaluated by subtracting the pellet initial weight (M_o) before immersion from the immersed pellet weight (M) and dividing by M_o.

$$\mu = \frac{(M - M_o) \times 10^{-3}}{M_o} \quad (1)$$

In Fig. 3, it can be seen that the pellet porosity continuously increased from about 70 to 380 mg g^{-1} with the Ppy concentration in the range 0–50 wt%. This phenomenon is probably due to the Ppy particular porous structure [17].

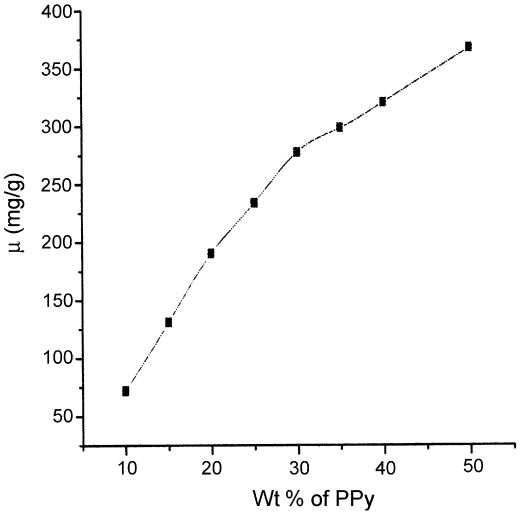

Fig. 3. Curve of the composite pellet porosity (μ) vs. the Ppy wt percentage. The porosity was measured after immersing the pellets in a 0.3 M $NaClO_4$ aqueous solution during 48 h.

It was also confirmed by comparing the SEM micrographs of pure graphite and of composite pellets containing Ppy concentrations of 10 and 40 wt% (Fig. 4). The surface morphology of pure graphite and composite pellets containing only 10% of Ppy was characterized by the very apparent presence of graphite layers in both materials (Fig. 4a and b). But, the Ppy globules located on graphite strips became much more numerous when the Ppy concentration was increased from 10 to 40% (Fig. 4b and c). Such a morphology, which corresponds to a relatively well-developed Ppy/graphite composite surface, seems very promising for the application of composite electrodes to the development of batteries and supercapacitors.

Moreover, the porous structure of Ppy powder and of pellets (composite electrodes) containing 0, 20 and 40 wt% of Ppy was also studied by the BET method. The BET surface area values were relatively close, ranging between 3.8 and 7.0 m^2 g^{-1}. The BET measurements of pore volume and size showed that, in fact, the material is constituted of particles which are in close contact, but do not possess any intrinsic microporosity. This suggests that the interfacial processes would occur according to two time scales: these taking place at the free surface of the particles would be relatively fast, whereas those implying a diffusion phenomenon inside the particles would have a very slow rate. In these conditions, our porosity measurements based on water retention represent the simplest and most convenient, experimental approach to determine the electrode porosity properties.

3.4. Electrochemical activity of Ppy/graphite composite electrodes

As already pointed out, one of the aims of this work was to electrochemically characterize the Ppy/graphite composite electrodes. Also, it is worthwhile to mention that the experimental data reported here concerned essentially half-cell systems. For the sake of clarity, the results of both electrochemical techniques (cyclic voltammetry and chronopotentiometry) used for characterization of the composite electrodes are discussed separately in the following parts, but they can be considered as complementary.

3.4.1. Cyclic voltammetry

The cyclic voltammograms (CVs) of a Ppy/graphite composite electrode (10 wt% in Ppy) were investigated in a 0.3 M $NaClO_4$ aqueous solution at various scanning rates ranging from 0.1 to 2.0 mV s^{-1} (Fig. 5). As can be seen, the oxidation and reduction peaks of the CVs are well defined, but broad and asymmetric, the separation between the peak potentials being relatively large ($\Delta E_p \approx 1.0$ V) and also depending on the scan rate. It has been suggested that the electrochemical charging/discharging process, i.e. the CV behavior of a redox composite electrode, might be influenced by the ohmic resistance [18,19]. The inset of Fig. 5 shows that the current densities of anodic and cathodic peaks linearly vary with the square root of the potential scan rate, which indicates that the redox reaction is controlled by the diffusion of anions through the porous composite electrode. Moreover, careful observation of the CV curves revealed the presence of high capacitive current

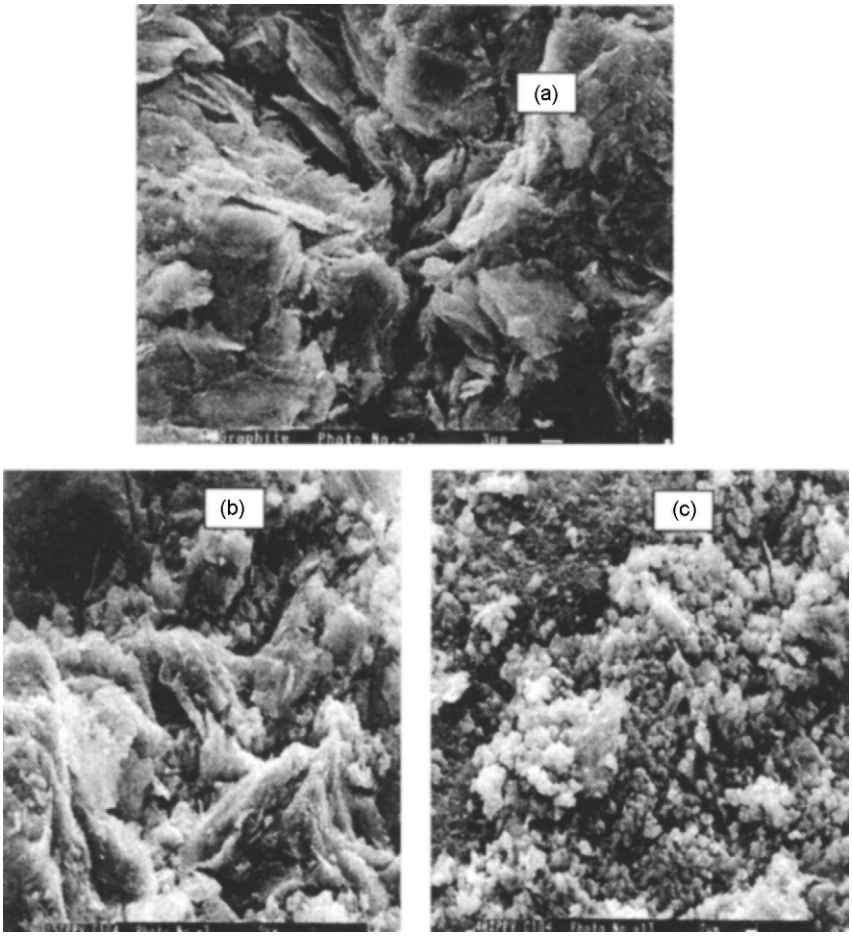

Fig. 4. SEM photos of: a graphite pellet (a) and composite pellets containing (b) 10 wt% of Ppy and (c) 40 wt% of Ppy.

values that are remaining even after the redox reaction has taken place.

The capacity values, calculated from the voltammograms of Fig. 5 – obtained for a composite electrode containing 10 wt% in Ppy – were relatively high, reaching, about 6 and 2 F, respectively, in the anodic and the cathodic domains, corresponding to a mean value of 20 F g^{-1} of electrode mass or 40 F cm^{-3}, the composite density being close to 2 g cm^{-3}. With respect to the only Ppy active mass, the mean capacity value is 0.2 F mg^{-1}, which compares favorably to the literature data reported for a pure Ppy electrode [15]. Such a behavior can be attributed to a pseudo-capacitance charging process, which would be occurring in the doped state [10,20]. Indeed, it appears that the oxidation current intensity value is higher than the reduction current one.

Moreover, the cyclic voltammogram of a pure graphite pellet was recorded. Our calculations of capacity, based on this voltammogram, led to a double-layer capacity value of 1.2 F g^{-1} of graphite, which corresponds, respectively, to a double-layer capacity graphite contribution of only about 5.4 and 0.9%, respectively, for composite electrode with 10 and 40 wt% Ppy content. Another interesting feature is that the redox peak surface of CVs was found to significantly increase with the Ppy amount, varying from 10 to 30% in the composite electrodes. In these conditions, the CVs (recorded at a 1 mV s^{-1} scan rate) also presented redox peaks with the same type of asymmetry and broadness at all Ppy concentrations under study. In addition, the capacitive current as well as the capacity values, increased linearly with the Ppy amount, a slope of 0.47 F cm^{-2} per percentage of Ppy being calculated for the anodic branch of the CVs (Fig. 6). This confirms that the double-layer capacity graphite contribution to the capacitive charge storage process can be considered as negligible relative to that of Ppy. Clearly, the total charging/discharging capacities depended on two simultaneous processes, including the faradic reaction (Eq. (2)) and the capacitive reaction occurring in the chemically synthesized Ppy structure.

$$[\mathrm{Py}]_x + xy\mathrm{A}^- \leftrightarrow [\mathrm{Py}^{y+}\mathrm{A}_y{}^-]_x + xye^- \quad (2)$$

where A^- is the anion, x the degree of polymerization ($10 < x < 1000$) [21] and y is the charge of one pyrrole repetitive unit (corresponding to the doping level with $y = 0.33$ in the case of chemical synthesis [15]).

3.4.2. Chronopotentiometry

The effect of the Ppy percentage on the discharging capacity was examined by recording the chronopotentiometric curves in composite electrodes, containing various Ppy concentrations in the range 10–70% (Fig. 7). Using an applied current density value of 1 mA cm^{-2}, the aspect of these curves was comparable to that of a typical capacitor [22].

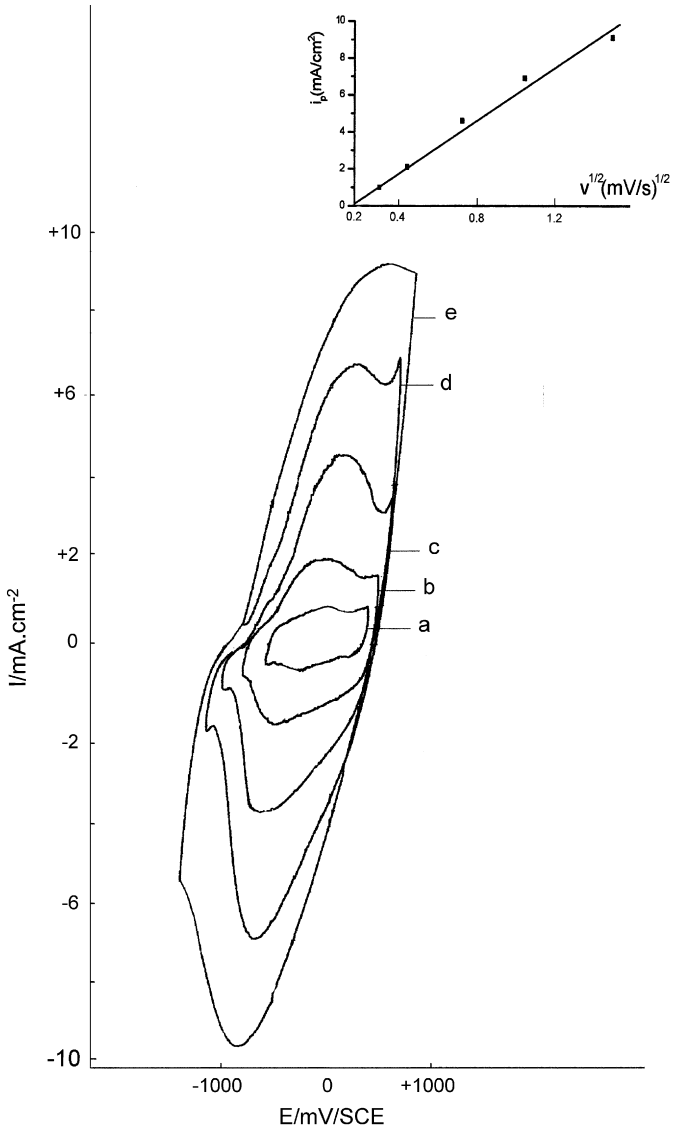

Fig. 5. Cyclic voltammograms of a Ppy (10 wt%)/graphite composite electrode in a 0.3 M $NaClO_4$ aqueous solution, recorded at different potential scan rates. The inset shows a linear plot of the anodic and cathodic peak current intensity vs. the scan rate square root. The scan rate values are, respectively: Curve a: 0.1 mV s^{-1}; b: 0.2 mV s^{-1}; c: 0.5 mV s^{-1}; d: 1.0 mV s^{-1}; e: 2.0 mV s^{-1}.

The resulting massic capacities Q (calculated from the chronopotentiometric curves of Fig. 7a and b) were plotted against the Ppy concentration (Fig. 8). As can be seen, the curve exhibited a Q maximum value of 99.6 mAh g^{-1} of Ppy for a 40 wt% Ppy. When the Ppy concentration exceeded this value, the massic capacity dramatically decreased, which can be explained by the resistance effect resulting from the densification of Ppy globules located on the graphite strips. In agreement with literature data [15], a significant discrepancy was found between the Ppy massic capacity theoretical (for a doping level of 0.33) and experimental values, which were, respectively, 88 and 99.6 mAh g^{-1} of Ppy. In the absence of overdoping, this observation strongly supports the hypothesis that the measured total charge partly corresponds to the faradic charging process and an associated capacitance effect possibly due to a ionic

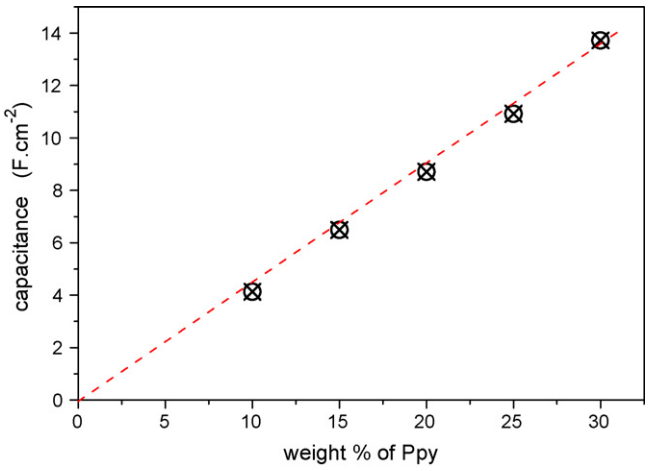

Fig. 6. Curve of the electrode capacitance vs. the Ppy wt percentage, estimated from the anodic part of the corresponding voltammograms.

displacement in the polymeric material, according to Eq. (3).

$$Q_t = Q_f + Q_c \quad (3)$$

where Q_t is the total massic capacity, Q_f the faradic massic capacity and Q_c is the interfacial capacitive contribution arising from both Ppy/electrolyte and graphite/electrolyte interfaces. Assuming that the Q_f maximum value corresponds to the faradic capacity theoretical value (88 mAh g^{-1}), it becomes clear that Q_c would represent approximately 11% of the total massic capacity. In addition, as shown in the following section, the EIS measure-

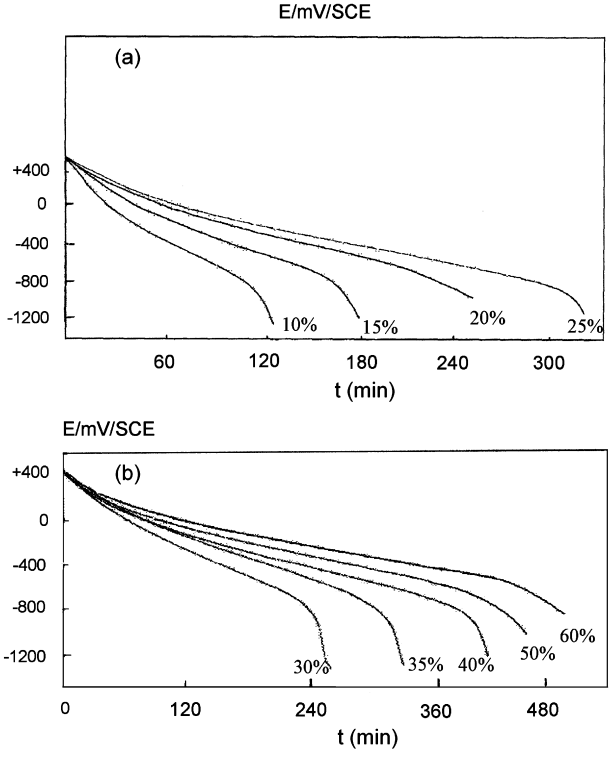

Fig. 7. Chronopotentiometric curves of Ppy/graphite composite electrodes in a 0.3 M $NaClO_4$ aqueous solution, obtained at wt percentages of Ppy varying from: (a) 10–25% and (b) 30–60%.

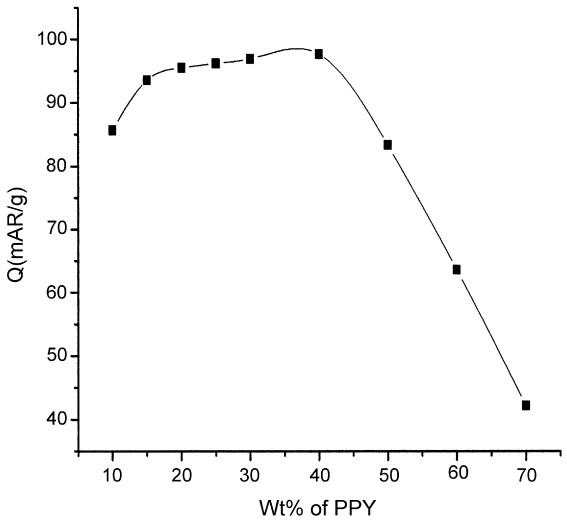

Fig. 8. Curve of the composite electrode massic capacity (Q) vs. the polypyrrole wt percentage.

ments also indicate that the capacitive contribution of graphite is negligible relative to that of the polymer.

3.4.3. Polarization curves and impedance measurements

In this EIS study, the Ppy content of the composite electrode was 40%, with a corresponding porosity of 320 mg g^{-1}. Its electrical resistivity was 1.4 Ω cm. Quasi-stationnary polarization curves are depicted in Fig. 9, obtained for a composite pellet containing 40 wt% of Ppy. Curves (1) and (2) correspond, respectively, to the current values recorded before and after impedance measurements. In the case of the anodic branch, the dc current was practically time independent. For the cathodic branch, a net decrease of the current was observed after the time elapsed for recording an impedance spectrum (about 35 min). The time dependence was practically identical, whatever was the cathodic potential value. Also, it is worthwhile to note that, after an impedance measurement sequence, the fact of changing the applied potential by 50 mV yielded a very quick increase of the cathodic current from the values of curve (1) towards those of curve (2).

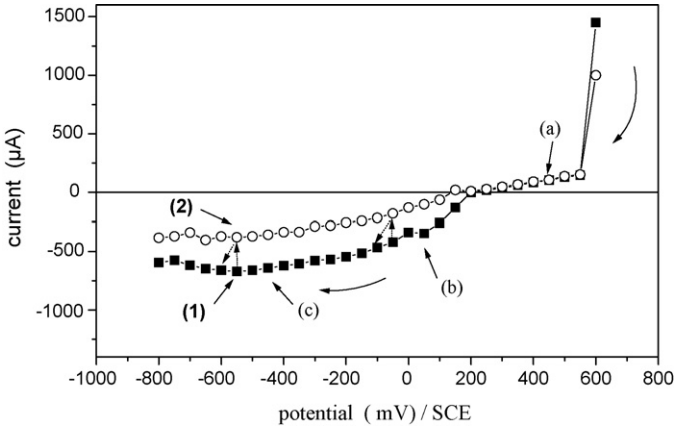

Fig. 9. Polarization curves obtained for a composite pellet containing 40 wt% of Ppy, (1) before and (2) after recording an impedance spectrum.

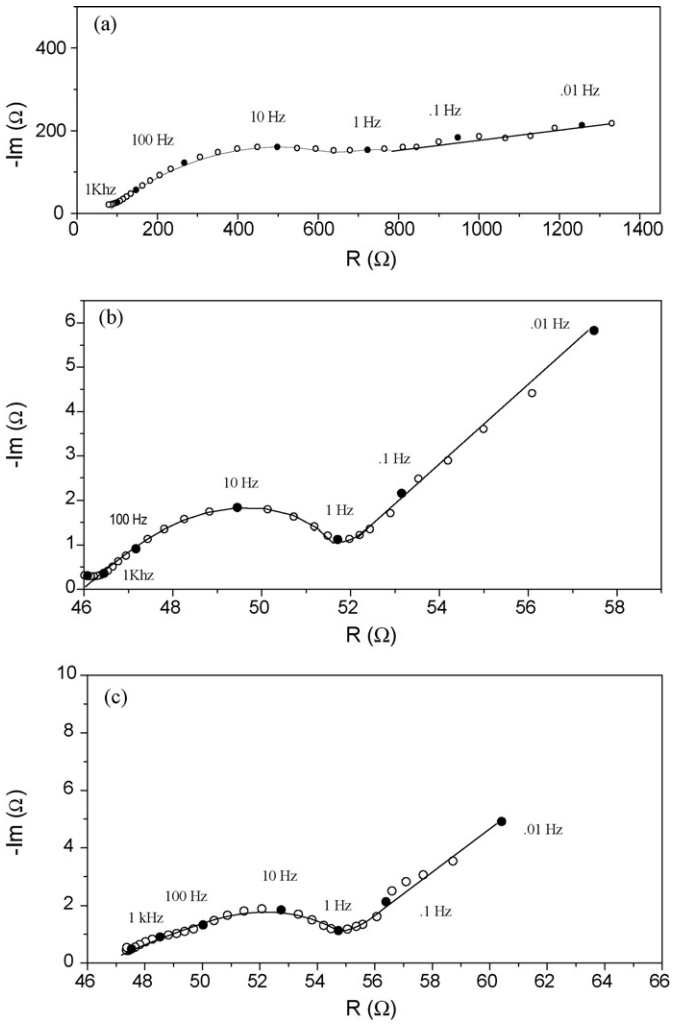

Fig. 10. Complex plane impedance plots obtained at various potentials: (a) +450 mV, (b) +100 mV and (c) −450 mV/SCE.

Some examples of electrochemical impedance spectra obtained at +450, +100 and −450 mV are given in Fig. 10a–c, in the Nyquist representation. Two capacitive contributions can be roughly identified over the entire potential domain under study. The main, more or less flattened loop represents the impedance response at mid- and high-frequencies, above about 1 Hz, with a maximum of its imaginary component at a frequency value close to 10 Hz in all cases. The high-frequency behaviour was characterized by a constant phase angle, which points out the porous character of the electrodes (transmission line behaviour). This angle value was equal to 45° (Fig. 10a and b), except at a large cathodic potential value (Fig. 10c), where it was only 22.5°, suggesting that, in the latter case, some additional diffusion phenomenon takes place in the porous material. In the low frequency domain, below 1 Hz, we observed a capacitive contribution which can be related to a diffusion process. The impedance values were larger in the anodic domain (Fig. 10a) than in the cathodic one (Fig. 10b and c), in agreement with the very different dc current values in each domain. It is important to note that, in the case of our composite electrodes, the low frequency limit of the Nyquist diagram, which is characterized by

a vertical line corresponding to the large pseudo-capacitance (a few Farads) of the electrode, was not reached. To reach this limit, it would be necessary to perform measurements at frequencies well below 1 mHz.

In a first approach, a quantitative analysis of these electrochemical impedance spectra can be carried out on the basis of an idealised, one-dimensional cylindrical pore model and a finite transmission line electrical model [23,24]. An analytical expression of the electrode impedance can be found in [24]. It has been tested experimentally for well-defined porous textures [25] as well as for particles of irregular shape [26], and can be used to estimate the average pore morphology. The impedance $Z(j\omega)$ is a complex function of several variables formally written as:

$$Z(j\omega) = R_e + f(l, r, n, \rho_s, \rho_m, R_w, C_w, \alpha_w, R_b, C_b, \alpha_b, V_p, \theta, \omega) \quad (4)$$

where l, r and n are, respectively, the length, radius and surface density of pores, ρ_s the electrolyte resistivity and ρ_m the material resistivity, R_w and C_w are, respectively, the transfer resistance and the double-layer capacity along the pore wall, at the graphite/Ppy/electrolyte interface. R_b and C_b are, respectively, the transfer resistance and the double-layer capacity at the bottom of the pore, i.e. at the rear contact/electrolyte/Ppy interface, α_w and α_b the dispersion coefficients, accounting for the flattening of the capacitive loops, R_e the electrolyte resistance, V_p the volume of electrolyte able to find a place between the graphite and the Ppy particles, and evaluated from porosity measurements and θ is the fraction of total surface area without emergent pores. The full expression of $Z(j\omega)$ is given in Appendix A.

The information concerning the porous electrode, i.e. the values of all the parameters involved in the expression of $Z(j\omega)$, has been derived through a non-linear curve fitting of Eq. (4) to ac impedance data in the frequency range 1 Hz–60 kHz. The fitting was conducted by using a non-linear least squares simplex procedure, assuming an accuracy of 1% on the impedance modulus. The fitting quality was appreciated by a dimensionless factor σ, defined as the standard deviation of the difference between the calculated and experimental values reduced to the experimental error. A good fitting quality would correspond to a σ factor value close to or less than unity.

An example of fitted curves is given in Fig. 11 for the data recorded at +100 mV. A satisfactory agreement between experimental and calculated data is obtained, indicating that the actual porous, composite electrode behaves well as an ideal cylindrical pore electrode. The values of the fitted parameters are gathered in Table 1. A V_p value of 0.0625 cm^3 was deduced from porosity experiments, and the α_w value was fixed at 0.9. Calculations show that a good fit can only be obtained by considering that l is of the order of magnitude of the actual electrode thickness. Moreover, the R_b and C_b values (Table 1) show that the total impedance is dominated by the interfacial impedance at the pore wall. From the calculated surface density value of pores $n = 4.4 \times 10^6$ cm^{-2}, it is possible to obtain the average pore radius and the active surface area of the composite electrode which are, respectively, 1.8 μm and 700 cm^2. The calculated

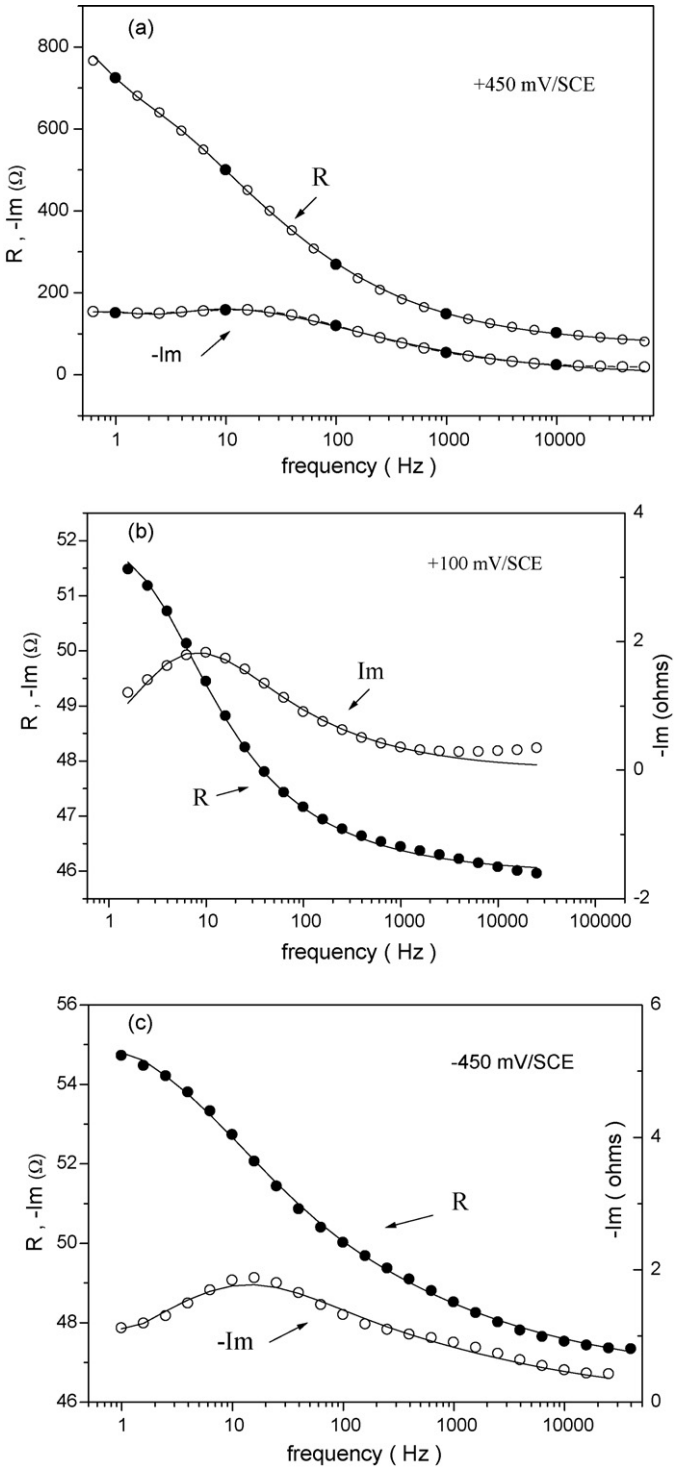

Fig. 11. Comparison of experimental and fitted data according to Eq. (4) in the Bode representation of the real (R) and imaginary (Im) parts: (a) +450 mV, (b) +100 mV and (c) −450 mV/SCE.

double-layer capacity at the interface graphite/Ppy/electrolyte being 17 μF cm^{-2}, the total capacity reaches a value of 11.9 mF, or 0.06 F g^{-1} with respect to the electrode mass. The latter capacity value represents less than 0.1% of that obtained from the voltammograms (80 F g^{-1} of electrode mass for the 40% Ppy containing electrode). This very low double-layer capacitance

Table 1
Fitted parameters obtained according to Eq. (4), and corresponding to the impedance spectrum recorded at +100 mV/SCE for a composite electrode containing 40% of Ppy in contact with a 0.3 M $NaClO_4$ aqueous solution

C_w[a] ($\mu F\,cm^{-2}$)	R_w[b] ($\Omega\,cm^2$)	α_w[c]	l[d] (cm)	V_p[e] (cm^3)	ρ_m[f] (Ω cm)	C_b[a] ($\mu F\,cm^{-2}$)	R_b[b] ($\Omega\,cm^2$)	α_b[c]	ρ_s[f] (Ω cm)	R_e[g] ($\Omega\,cm^2$)	n[h] (cm^{-2})
17	1940	0.9	0.14	0.0625	1	∞	5	1	34	46	4.4×10^6

[a] $C_w(C_b)$, double-layer capacity along the pore wall (at the bottom of the pore).
[b] $R_w(R_b)$, transfer resistance along the pore wall (at the bottom of the pore).
[c] $\alpha_w(\alpha_b)$, dispersion coefficient of the wall impedance (of the bottom impedance).
[d] l, length of pores.
[e] V_p, volume of the pores.
[f] $\rho_m(\rho_s)$, material (electrolyte) resistivity.
[g] R_e, electrolyte resistance.
[h] n, surface density of pores.

value, estimated by impedance measurements at high frequencies, reflects relatively fast charge relaxation effects, occurring essentially at the electrode surface.

In the cathodic domain, an additional diffusion phenomenon has to be taken into account to explain the 22.5° phase angle value observed at high frequencies. According to literature, this phenomenon could arise from the diffusion of ClO_4^- ions, very closely trapped in the Ppy polymer chains [27]. For instance, the electrochemical impedance spectrum recorded at −450 mV was well described using Eq. (4), by taking an α_w value of 0.5, and a quality factor value of 0.2. These results suggest that, in all cases, the composite electrode can be described by the cylindrical pore model.

This model can also be applied to the anodic domain. By fixing the l and n values reported in Table 1, it is possible to obtain a good fit of the experimental impedance spectrum recorded at +450 mV. The main feature is that the transfer resistance is very large (a few MΩ). These results show that the composite electrode is poorly active in the anodic domain. Since Ppy is a p-type semi-conducting polymer in the oxidized state, it can be assumed that the composite electrode becomes electrochemically inactive because of a saturation of the polymer structure by the anions.

From the standpoint of EIS analysis, and considering the frequency range under study and the respective time scales of the processes taking place at the graphite/electrolyte and Ppy/electrolyte interfaces, only the effects of double-layer charging at the graphite/electrolyte interface have been observed. Therefore, the profile of the impedance diagrams can be related to the macroporous structure of the composite electrode.

4. Conclusion

In the present work, we have been able to build large size composite electrodes, containing chemically synthesized polypyrrole powder and graphite carbon in various percentages, and we have characterized in detail their morphological and electrochemical characteristics. We have demonstrated that our method of preparation of the composite pellets provided a material with satisfactory conductivity and porosity values. It is worthwhile to stress that such physico-chemical properties are highly favorable for applications to batteries and supercapacitors. Also, our morphology study revealed the presence of two distinct pore systems in the composite pellets, including micropores, derived from the Ppy peculiar, porous structure and macropores due to the spaces located between the graphite strips.

Using the cyclic voltammetry method, we have shown the existence of a capacitance effect, characteristic of the polypyrrole oxidized state. The latter result was confirmed by chronopotentiometric experiments which indicated that the capacitive effect contribution represented about 11% of the total massic capacity in the composite electrodes. Moreover, this phenomenon might explain the massic capacity high value obtained in charge–discharge tests.

The electrochemical impedance spectrometry measurements, performed within a wide potential range, indicated that it was possible to describe the composite electrodes by the cylindrical pore model. In the frequency range under study, when taking into account the relative time scales of the processes at the graphite (fast) and Ppy (slow) interfaces, only the effects of double-layer charge at the electrode/electrolyte interface are observable. It was concluded that the capacitive contribution of graphite was at the most 1% of the total electrode capacitance. In contrast, the CV study has shown that these composite electrodes possess high massic capacity values of approximately several hundreds of $F\,g^{-1}$ of Ppy mass, corresponding to the electrical charges stored in Ppy. At high cathodic potential values, the impedance measurements allow one to establish a relationship between the decrease of double-layer capacity and the rearrangement of charges, implying the diffusion of ClO_4^- anions close to the polymer chains in the composite electrodes.

Overall, our work strongly suggests that a composite electrode, prepared by our method and containing chemically synthesized polypyrrole powder and graphite carbon in appropriate percentages, could be used as one half-cell in a super-capacitor, after thorough optimization of the composite material porosity.

Acknowledgements

We gratefully acknowledge the French Ministry of Foreign Affairs for having provided, in part, the financial support of this work (French-Senegalese CAMPUS Project No. 99 317 102, 1999–2004).

We also warmly thank Dr. C.M. Pradier, Dr. J. Blanchard and Ms. C. Boucher (Laboratoire de Réactivité de Surface, UMR

7609 CNRS, University of Paris 6) for their help in performing the BET measurements on our samples.

Appendix A

The impedance analysis of the composite electrodes is based on a one-dimensional cylindrical pore model and a finite transmission line electrical model. The involved parameters are defined in the text and in the caption of Table 1. The composite electrode is modelled as the parallel combination of parallel cylindrical pores, of length l, radius r and surface density n. The electrode resistance R_w and solution resistance R_s per pore length unit are, respectively, given by Eqs. (A1) and (A2):

$$R_w = \frac{\rho_m n}{\theta} \tag{A1}$$

$$R_s = \frac{\rho_s}{\pi r^2} \tag{A2}$$

where θ is the volume fraction occupied by the composite material, with resistivity ρ_m and ρ_s is the electrolyte resistivity. θ is calculated from the pore volume V_p as:

$$\theta = 1 - \frac{4V_p}{\pi l D^2} \tag{A3}$$

where D is the electrode diameter. The pore density n is then deduced from θ by considering the pore surface occupancy:

$$1 - \theta = n\pi r^2 \tag{A4}$$

The interfacial impedance of the pore wall per unit of length is given by Eq. (A5):

$$Z_w = \frac{R_w}{[1 + (jR_wC_w\omega)^{\alpha_w}]2\pi r} \tag{A5}$$

and that of the pore bottom by Eq. (A6):

$$Z_b = \frac{R_b}{[1 + (jR_bC_b\omega)^{\alpha_b}]\pi r^2} \tag{A6}$$

where C_w and C_b are the double-layer capacitances, respectively, along the wall and at the bottom of the pore. The impedance of a pore Z_p is given by Eq. (A7):

$$Z_p = \frac{R_m R_s l}{R_m + R_s} + \frac{2R_m R_s + (R_m^2 + R_s^2)\cosh(l/\lambda) + \lambda\delta R_s^2 \sinh(l/\lambda)}{(R_m + R_s)[\delta \cosh(l/\lambda) + \lambda^{-1} \sinh(l/\lambda)]} \tag{A7}$$

where λ is the penetration depth:

$$\lambda = \sqrt{\frac{Z_w}{R_m + R_s}} \tag{A8}$$

and δ corresponds to:

$$\delta = \frac{R_m + R_s}{Z_b} \tag{A9}$$

The n pores are assumed to be in parallel, and the final porous electrode impedance Z_P per surface unit is given by:

$$Z_P = \frac{Z_p}{n} \tag{A10}$$

The complete impedance expression to be compared to experimental data in the frequency range 62 kHz–1 Hz reads:

$$Z(j\omega) = R_e + Z_P \tag{A11}$$

References

[1] F.R. Kalhammer, Solid State Ionics 135 (2000) 315–323.
[2] K.S. Ryu, Y. Lee, K.S. Han, M.G. Kim, Mater. Chem. Phys. 84 (2004) 380–384.
[3] G. Sandi, K.A. Carrado, H. Joachim, W. Lu, J. Prakash, J. Power Sources 119–121 (2003) 492–496.
[4] R. Sivakumar, R. Saraswathi, J. Power Sources 104 (2002) 226–233.
[5] P.G. Bruce, Chem. Commun. 19 (1997) 1817–1824.
[6] J.R. Owen, Chem. Soc. Rev. 26 (1997) 259–267.
[7] E. Frackowiak, F. Beguin, Carbon 39 (2001) 937–950.
[8] B. Veeraraghavan, J. Paul, B. Haran, B. Popov, J. Power Sources 109 (2002) 377–387.
[9] J. Fan, M. Wan, D. Zhu, B. Chang, Z. Pan, S. Xie, Synth. Met. 102 (1999) 1266–1267.
[10] A. Rudge, J. Davey, I. Raistrick, S. Gottesfeld, J. Power Sources 47 (1994) 89–107.
[11] A. Rudge, I. Raistrick, S. Gottesfeld, J.P. Ferraris, Electrochim. Acta 39 (1994) 273–287.
[12] K. Jurewicz, S. Delpeux, V. Bertagna, F. Béguin, E. Frackowiak, Chem. Phys. Lett. 347 (2001) 36–40.
[13] M.H. Hughes, G.Z. Chen, M.S.P. Shaffer, D.J. Fray, A.H. Windle, Chem. Mater. 14 (2002) 1610–1613.
[14] J.H. Park, J.M. Ko, O.O. Park, D.W. Kim, J. Power Sources 105 (2002) 20–25.
[15] N. Mermilliod, J. Tanguy, F. Petiot, J. Electrochem. Soc. 133 (1986) 1073–1079.
[16] J. Stejskal, M. Omastova, S. Fedorova, J. Prokes, M. Trchova, Polymer 44 (2003) 1353–1358.
[17] H. Zhao, W.E. Price, G.G. Wallace, J. Membr. Sci. 148 (1998) 161–172.
[18] C.P. Andrieux, J.M. Saveant, J. Electroanal. Chem. 111 (1980) 377–381.
[19] S. Stankovic, R. Stankovic, M. Ristic, O. Pavlovic, M. Vojnovic, React. Funct. Polym. 35 (1997) 145–151.
[20] G.A. Snook, G.Z. Chen, D.J. Fray, M. Hughes, M. Shaffer, J. Electroanal. Chem. 568 (2004) 135–142.
[21] A.F. Diaz, J. Bargon, in: T.A. Skotheim (Ed.), Handbook of Conducting Polymers, vol. 1, Marcel Dekker, New York, NY, 1986, p. 81.
[22] Y. Kibi, T. Saito, M. Kurata, J. Tabuchi, A. Ochi, J. Power Sources 60 (1996) 219–224.
[23] R. de Levie, in: P. Delahay (Ed.), Advances in Electrochemistry and Electrochemical Engineering, vol. IV, Interscience, New York, 1967, p. 329.
[24] J.R. Park, D.D. Macdonald, Corros. Sci. 23 (1983) 295–315.
[25] J.P. Candy, P. Fouilloux, M. Keddam, H. Takenouti, Electrochim. Acta 26 (1981) 1029–1034.
[26] C. Cachet, R. Wiart, J. Zoppas-Ferreira, Electrochim. Acta 38 (1993) 311–318.
[27] J. Tanguy, N. Mermilliod, M. Hoclet, J. Electrochem. Soc. 134 (1987) 795–802.